Journal of
Sensor and Actuator Networks

MDPI

Review

Bluetooth Communication Leveraging Ultra-Low Power Radio Design

Omar Abdelatty, Xing Chen, Abdullah Alghaihab and David Wentzloff *

Department of Electrical Engineering, University of Michigan, Ann Arbor, MI 48109, USA; omaratty@umich.edu (O.A.); chenxing@umich.edu (X.C.); abdulalg@umich.edu (A.A.)
* Correspondence: wentzlof@umich.edu

Abstract: Energy-efficient wireless connectivity plays an important role in scaling both battery-less and battery-powered Internet-of-Things (IoT) devices. The power consumption in these devices is dominated by the wireless transceivers which limit the battery's lifetime. Different strategies have been proposed to tackle these issues both in physical and network layers. The ultimate goal is to lower the power consumption without sacrificing other important metrics like latency, transmission range and robust operation under the presence of interference. Joint efforts in designing energy-efficient wireless protocols and low-power radio architectures result in achieving sub-100 μW operation. One technique to lower power is back-channel (BC) communication which allows ultra-low power (ULP) receivers to communicate efficiently with commonly used wireless standards like Bluetooth Low-Energy (BLE) while utilizing the already-deployed infrastructure. In this paper, we present a review of BLE back-channel communication and its forms. Additionally, a comprehensive survey of ULP radio design trends and techniques in both Bluetooth transmitters and receivers is presented.

Keywords: Bluetooth Low-Energy (BLE); Internet-of-Things (IoT); back-channel communication; star network; ultra-low power; radio design trade-offs; wakeup receiver

check for updates

Citation: Abdelatty, O.; Chen, X.; Alghaihab, A.; Wentzloff, D. Bluetooth Communication Leveraging Ultra-Low Power Radio Design. *J. Sens. Actuator Netw.* **2021**, *10*, 31. https://doi.org/10.3390/jsan10020031

Academic Editor: Atis Elsts

Received: 16 February 2021
Accepted: 19 April 2021
Published: 26 April 2021

Publisher's Note: MDPI stays neutral with regard to jurisdictional claims in published maps and institutional affiliations.

Copyright: © 2021 by the authors. Licensee MDPI, Basel, Switzerland. This article is an open access article distributed under the terms and conditions of the Creative Commons Attribution (CC BY) license (https://creativecommons.org/licenses/by/4.0/).

1. Introduction

Bluetooth Low-Energy (BLE) is the leading protocol for short-range, low power wireless communication networks [1]. Wireless short-range technologies like BLE support tens of meters of maximum distance between devices for a variety of applications including wireless sensor networks and the majority of the low-power devices used in the Internet of Things (IoT) (Figure 1a). The BLE standard has a competitive advantage over other IoT-compatible wireless technologies because of its ability to communicate directly with smart phones, computers and tablets. Since consumer electronics are ubiquitous, BLE-enabled IoT devices can be seamlessly connected to personal area networks without the need for additional wireless access points. The use cases for BLE have proven to be valuable in different IoT applications including medical health monitoring, automated emergency calls, smart tags, home automation and in-vehicle networks. For environmental and industrial monitoring systems, BLE beacon tags can also be used for indoor localization [2,3], identification and tracking of objects and personnel.

In such applications, the power consumption of the device is widely recognized as the limiting factor to scaling the number of battery-powered IoT devices [4]. Assuming a scenario where a billion devices are deployed with an expected battery lifetime of 1 year, this would result in replacing 2.7 million batteries each day. In reality, this unacceptable number imposes significant logistical burdens in operational deployments and reduces the utility of IoT devices in different sectors. Batteries represent a logistically prohibitive maintenance problem that requires a large maintenance workforce, presenting a daunting challenge for individual facilities where maintenance resources are already at capacity. Therefore, the battery is needed to last as long as the life of the product, which can be on the order of 10 years for an embedded device performing signal processing and wireless

communication [5]. Current battery lifetimes of BLE sensors are typically <1 year, far short of the 10-year target for other IoT protocols such as cellular narrowband IoT (NB-IoT) and LoRa devices. However, reducing the power consumption and the operating supply voltages enable the design of self-powered IoT devices in which energy harvesting technologies can be used to power the node from the environment [6]. One growing application in this field is body-powered wearable devices in mobile health technologies which allow remote and continuous health monitoring as shown in Figure 1b [7]. Another application in the industrial sector is in machine health monitoring (MHM), where self-powered ULP sensors can be deployed to observe specific abnormal patterns in the monitored physical/mechanical signals of a machine for early failure detection. Low-power operation facilitates harvesting of the machine's vibrational energy using piezo-electric materials to charge super-capacitors which are used to power the sensor [8].

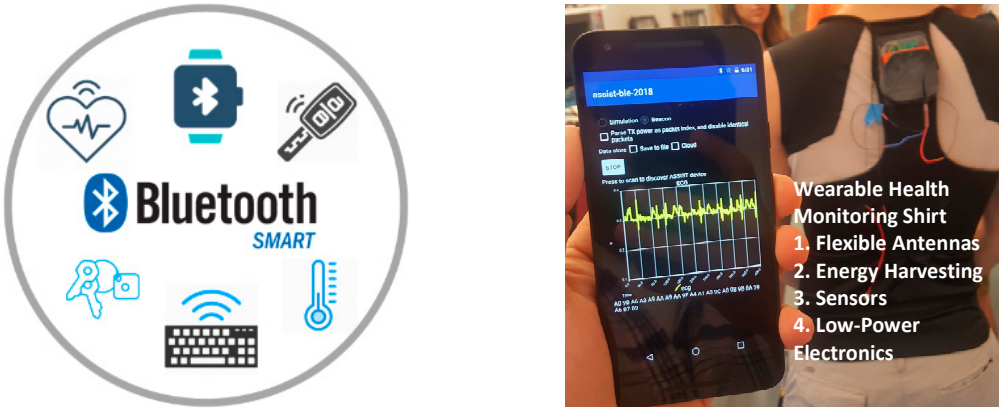

(**a**) (**b**)

Figure 1. (**a**) Wide range of consumer IoT applications, (**b**) self-powered wireless sensor systems used in health monitoring purposes.

Typically, the RF radio accounts for a significant portion of the aggregate power profile of the device. Thus, each data transmission operation performed by a battery-powered node shortens its subsequent lifetime, limiting the amount of data transmittable before needing to recharge/replace the battery. In a typical IoT application, it is reasonable to assume the radio consumes 60–90% of the operating power budget [9]. The active power for a single BLE packet transmission is usually several mWs, in addition to the startup energy of the frequency synthesizer and the crystal oscillator [10]. In order to extend the battery's lifetime, aggressive duty-cycling can be implemented [5]. This technique leads to a significant increase in the operational lifetime for battery-powered devices. Using the advertising interval (TI) defined as the time between two successive transmission events, the intended battery lifetime can be estimated (preferably >10 years). A good example application is a tracking device that establishes a Bluetooth connection to a smartphone. Using a common CR2031 coin battery with an energy density of 653 mWh, the required average power consumption for a 20-year lifetime is 3.7 µW and the TI can be calculated as shown in Figure 2. For a more accurate estimation, several additional factors need to be considered including: (1) the battery self-discharge rate (usually <20 years), (2) the battery capacity degradation by temperature variations and (3) the startup/shutdown overhead energy which might add extra ~50% to the power budget. All the aforementioned factors will limit the device from achieving the desired lifetime values.

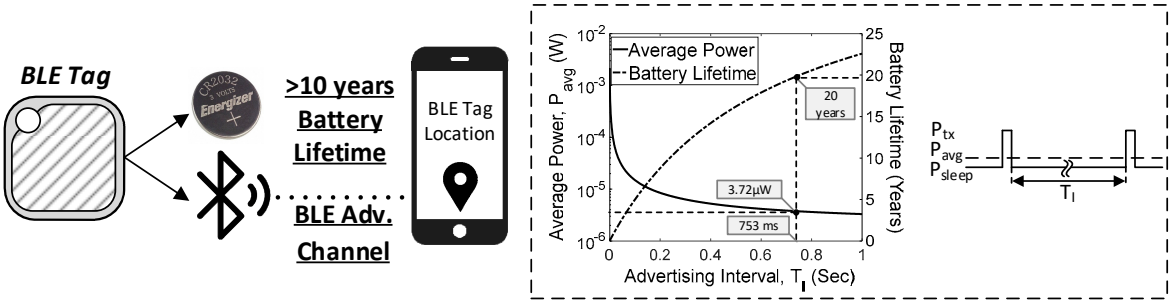

Figure 2. A typical IoT BLE application (**left**), the tradeoff between the required average power consumption and battery's lifetime in duty-cycled transmission targeting a specific latency (**right**).

This paper presents a review of recent efforts devoted to realizing low power connectivity solutions for wireless sensor nodes in BLE networks. The proposed solutions can be classified into two main categories: low-power radio design (physical layer) and energy-efficient wireless access technologies (network layer). Ultimately, combining the efforts in both areas will result in a new generation of IoT devices that are mobile and self-powered to help propel IoT applications to new paradigms.

The rest of the paper is organized as follows: in Section 2, we discuss different synchronization schemes adopted in IoT applications with the main focus on BLE networks. Then, we present the concept of asymmetric BLE communication, referred to as back-channel communication. A design example of a BC receiver is also described, demonstrating one possible implementation of the BC communication in BLE-based networks. Section 3 reviews the ULP radio design challenges and trade-offs in both receivers and transmitters. A summary of the state-of-the-art fully compliant and back-channel BLE radios is reported, emphasizing the trade-off between the power consumption and other performance metrics. Finally, conclusions and future directions are presented in Section 4.

2. Back-Channel Communication for Energy-Efficient Operation

2.1. Synchronization Scehmes

The core operation of a wireless sensor node is to sense different physical phenomena from the ambient environment and share the information securely with other nodes within the network. Therefore, the IoT connectivity landscape is structured in the form of hierarchical layers of networking [11]. Local area networks are utilized to facilitate interaction between different nodes in the form of machine-to-machine (M2M) communication as well as establishing connection with the hub or the access point. Eventually, the access point (AP) sends the aggregated information from the endpoint nodes to the backend analytic engines to handle the event through means of wide area networks, mainly the internet. Based on the targeted application, the wireless connectivity capabilities of each sensor node is determined whether to stay online for continuous data exchange or in a "bursty" nature at scheduled/specific events. Many key performance factors regulate the design of the network like the latency budget, power consumption budget and capacity of the network. For short-range networks, usually a star topology is prevalent as seen with Bluetooth and body area networks. In a star topology, a set of endpoints are allowed to communicate only with a single controller (base station/access point), for example a smart phone.

Reliable network synchronization is needed for wireless sensor networks. It is a prerequisite to establish node-to-node and node-to-AP communication and is commonly performed in a controller-agent manner. However, the synchronization process might dominate power consumption when designing low-power radios for IoT. Two major application-specific synchronization schemes are proposed, resulting in different complexity and power budget requirements as summarized in Figure 3 [12]. In the first scheme, both the node and the AP radios keep transmitting the synchronization sequences (beacons) periodically. This approach offers the shortest network latency at the cost of increased power consumption due to the always-on radios. To achieve energy-efficient operation at

the battery-powered node, the radio is placed in a "sleep mode" to preserve the battery's lifetime. A separate ULP wake-up receiver (WuRx) can be designed to off-load the synchronization task from the main radio. The WuRx continuously searches for a pre-defined wakeup signal or the standard beacon from the AP. Once received, the WuRx will wake-up the main radio to perform on-demand high data-rate communication. Alternatively, in the asynchronous scheme, the node's radio is woken up only when needed asynchronously. The AP repeats transmitting the synchronization sequences until it acquires the node.

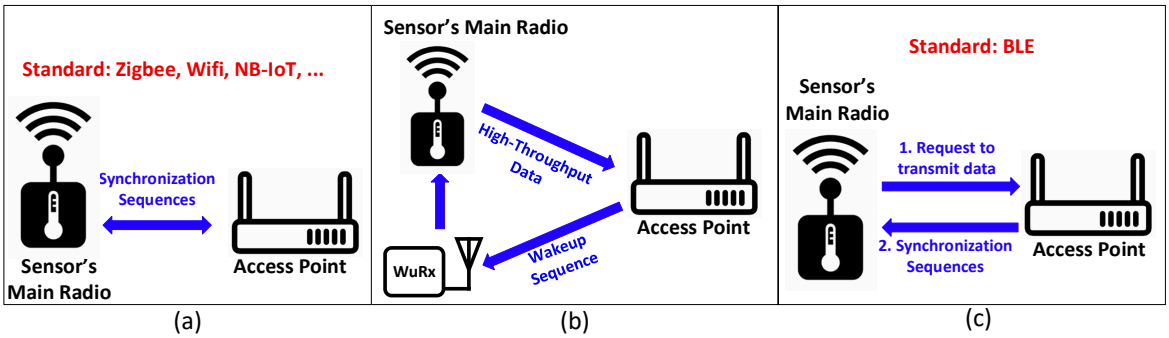

Figure 3. Different synchronization schemes resulting in different complexity and power budget requirements: (**a**) synchronous; (**b**) wake-up receivers; (**c**) asynchronous.

The WuRx receiver is an attractive solution to minimize the power consumption of the nodes while not compromising latency or scalability. The average power effectively becomes the active power of the always-on WuRx in addition to the leakage power of the main radio in a deep sleep mode. Since the WuRx and the main radio share the same communication link budget with the AP, both radios need to have similar sensitivity levels in order not to jeopardize the performance of the main radio. The reliability of the WuRx to properly detect the wakeup signaling in the presence of interference in congested bands is also of concern to minimize false alarms. Lastly, it is preferable for the WuRx signal sequence to be compatible with the communication protocol utilized in the network between the main radio and the AP to avoid additional hardware and cost at the AP side.

2.2. Back-Channel Communication Concept

Much research has been devoted to realizing energy-efficient wireless connectivity considering both the radio architectures and networking topologies. The motivation is to realize lasting operation for both battery-powered and battery-less wireless sensor nodes. According to the ULP radio survey [13], low power operation can be achieved when using simpler modulation techniques like on-off keying (OOK) or frequency-shift keying (FSK) at low data rates. Low complexity modulation schemes eliminate the requirement for having high-accuracy frequency synthesizers (PLL) which typically consume more than 50% of the radio power consumption. Moreover, lower data rates result in a lower SNR requirement and higher sensitivity level which can be achieved with basic radio architectures utilizing passive RF frontends [12]. The majority of previous work in this area utilizes simpler receiver architectures that rely on energy-detection and can achieve sub-10 µW active power consumption. However, it is difficult for these receivers to operate reliably in the presence of interference. Another challenge is that most of the wireless standards commonly used in IoT connectivity do not support such modulation techniques and data rates. For instance, the BLE standard utilizes Gaussian Frequency Shift Keying (GFSK) modulation with data rates of 1 or 2 Mbps. Although BLE signals are widely used in developed high population density areas, most ULP devices cannot take advantage of BLE connectivity because of their extremely limited power and/or complexity budget. State-of-the-art BLE radios still consume several mWs of active power. One reason behind the high power operation is the interference mitigation techniques to robustly achieve the highest possible sensitivity and adjacent channel rejection (ACR) performance. Efficient

techniques such as asymmetric BLE communications, duty-cycling, wakeup techniques, ring-oscillator-based local oscillator (LO) generation and open loop GFSK modulation have been reported to reduce the power consumption of the radio. Although heavy duty-cycling brings the average power down to sub-100 µW, it comes at the expense of long latency.

In this section, we will focus on BLE with back-channel communication. Prior work has reported the idea of back-channel communication, where signals are embedded in standard compliant wireless packets and generated by a standard-compliant transmitter [4,14–16]. The basic idea is to design ULP radios that are compatible but not fully-complaint with the BLE standard to encode information in an auxiliary low-complexity and low data rate modality as depicted in Figure 4. Two classes of IoT devices are considered: BLE-enabled (e.g., smart watch) devices where the power consumption is in the range of mW and ULP IoT devices (e.g., temperature sensors) with limited power consumptions of tens of µW. In such scenarios, commercial smart phones can be easily configured to transmit BLE back-channel messages in addition to the fully compliant BLE packets based on the targeted device. In back-channel communication, some BLE standard requirements like data rate can be traded off with power consumption while being able to still communicate properly with already deployed hardware infrastructures. Thus, the major advantage of this technique is that it leverages widespread smart phones to send back-channel signals which can be utilized in different applications scenarios. BLE back-channel communication can be seen as a wakeup mechanism that bridges the gap between ULP and standard compliant BLE radios. The BLE receiver stays in sleep mode until it is woken up through an always-on ULP WuRx listening to the back-channel to realize the concept of BLE on-demand. This approach significantly decreases the active power consumption of the receivers without sacrificing the latency in the network.

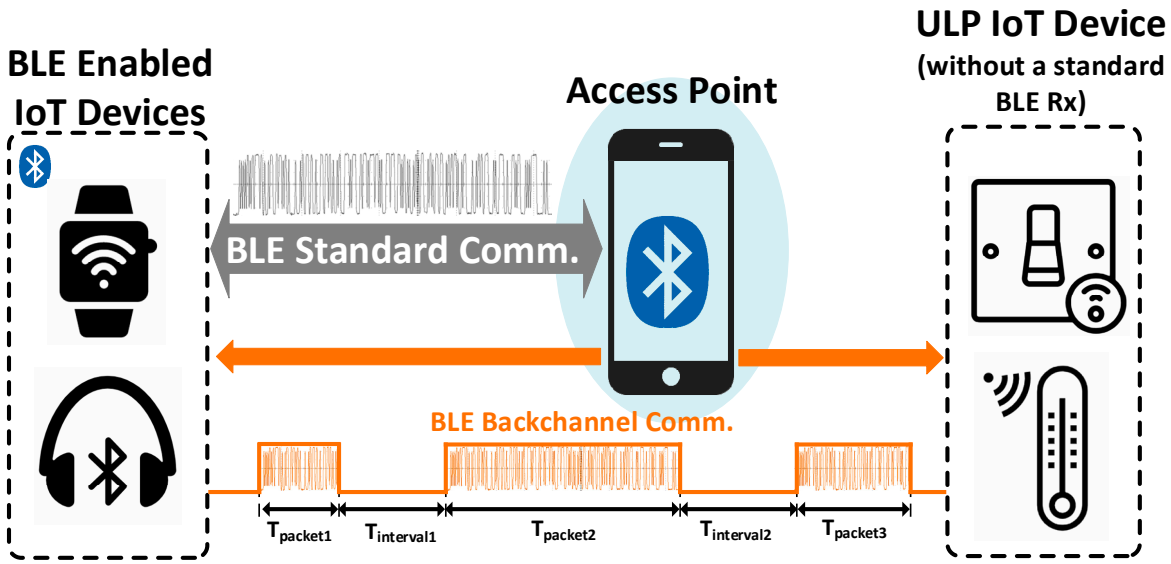

Figure 4. Concept of BLE (Bluetooth Low-Energy)-based back-channel communication.

One of the greatest challenges in designing an IoT platform is dealing with the heterogeneity of devices [4,14]. The proposed back-channel communication technology breaks this barrier to allow heterogeneous ULP IoT devices to interoperate with already existing BLE infrastructure with minimal power consumption [12]. The concept of embedded back-channel communication enables a variety of new applications with interconnecting heterogeneous devices. For example, the proposed scheme allows ULP devices in deep-sleep states that are not BLE compliant to wake up by back-channel communication embedded in standard BLE compliant packets.

Back-channel modulation is an entirely software-defined process which is accomplished by the MAC layer. It can be realized within a packet by generating a specific

sequence of bits in the payload [4] or applying duty cycling at the bit-level [17,18]. In addition, back-channel communication can be implemented on a packet-level by generating a proper sequence of packets [12,16]. Prior works [19,20] demonstrated the back-channel communication concept in the form of packet length modulation or packet interval modulation using multiple consecutive BLE packets as shown in Figure 4. The packet length or interval modulation utilizes an entire packet (or multiple packets) as an on-off-keying information symbol for an energy-detector based receiver. Its bandwidth efficiency, however, is very poor since the signaling requires many consecutive packets. Moreover, this form of back-channel signaling is particularly vulnerable to interferences as the packet length modulation is susceptible to an interferer packet (or any other high power interference signal) that could appear between multiple back-channel signaling packets. The other related technique is hierarchical modulation. In hierarchical modulation, receivers can selectively demodulate high rate (e.g., 16QAM) or low rate (e.g., 4QAM) information from a single packet depending on the channel quality. However, this hierarchical modulation scheme does not allow communication among heterogeneous devices using very distinct modulation schemes (e.g., coherent vs. non-coherent). Other work demonstrated intra-packet back-channel modulation schemes and the feasibility of the embedded back-channel signal generation without modifying the existing packet structure. Embedded back-channel signals are all generated by a set of carefully crafted bit sequences within the boundary of the standard-compliant packet structure. More specifically, binary FSK modulated back-channel communication embedded in GFSK BLE packets has been reported. A standard compliant data receiver can demodulate the entire bit sequence including the bits to create a back-channel message. Meanwhile, at the ULP back-channel receiver, only the embedded back-channel message is decodable, not the entire bit sequence. The backchannel signaling must be accomplished within strict constraints of the standard compliant packet structure.

2.3. ULP Back-Channel BLE RX Prototype

In order to further clarify the concept of back-channel communication and its implementation in the BLE standard, a BC receiver prototype is presented in this subsection. The receiver consumes 150 μW and is based on a ring oscillator (RO) for LO generation. The RO-based LO is designed to operate at 0.5× the BLE frequency band to reduce the active power consumption [16]. A dual-mixer front-end is hence required to enable the lower frequency for the oscillator. In this receiver, interference rejection is enhanced by (1) using a Zero-IF architecture to eliminate the image problem, (2) utilizing a narrowband low-pass filter at baseband with cutoff frequency of 1 MHz and (3) forming a 2-D backchannel message built on the presence and length of packets in all three advertising channels instead of utilizing a single advertising channel. This improves its resilience to interference. The FSK demodulation is performed by sensing the frequency-hopping sequence on the advertising channels. The frequency-hopping sequence can be defined in any order and still be compliant with the BLE standard. Therefore, this BC receiver can receive a wake-up message from a mobile phone that is sending a BLE compatible message.

A BLE advertising event includes three packets separated by less than 10 ms as shown in Figure 5. Each of these packets can be transmitted on any of the three BLE advertising channels which are numbered: CH37, CH38 and CH39. These channels' frequencies are 2402, 2426 and 2480 MHz, respectively. The packet duration can be anywhere between 128 to 376 μs (Figure 5 shows a 300 μs packet for illustration). The BLE standard specifies the time gap between advertising events to be at least 20 ms, but not more than 10.24 s. On top of this time gap, a pseudo-random delay of up to 10 ms is added to reduce the probability of collisions.

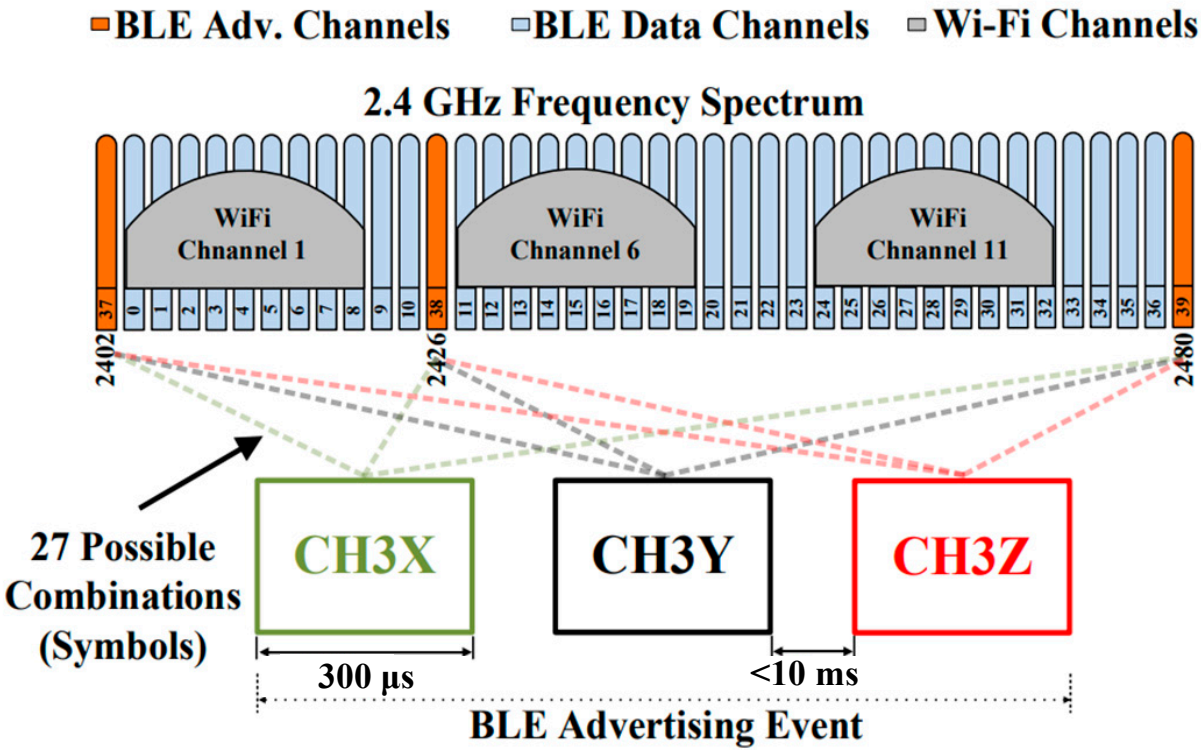

Figure 5. Structure of a BLE advertising event.

In the form of back-channel BLE communication used by this receiver, the three BLE advertising channels are scanned for the presence of transmitted energy. This is implemented by scanning the three channels sequentially for energy. To suppress the impact of adjacent channel interference, the bandwidth of the receiver baseband is set to 1 MHz. The receiver's oscillator frequency controller hops the oscillator frequency between all three BLE advertising channels (78 MHz apart).

This BC-BLE receiver was fabricated in a 65 nm LP CMOS process. At a 112.5 kbps data rate, the measured receiver sensitivity was -57.5 dBm for a 0.1% bit error rate (BER) requirement. To characterize the interference rejection of the receiver, a GFSK-modulated interferer is utilized in measurements. The signal-to interference ratio (SIR) was measured to be -4, -20 and -30 dB for the 1st, 5th and 10th BLE adjacent channels, respectively which is measured when the received signal amplitude is 3 dB higher the sensitivity level. The entire receiver consumes 150 µW total power from two separate supplies: 0.9 V for digital circuits and 1.1 V for analog blocks. About 120 µW (80%) is consumed by the RO-based LO generation including the LO buffers which operate at 1.2 GHz, the digital FLL and the LO frequency dividers. The remaining 30 µW is dissipated in the analog baseband.

3. BLE Radio Design Trends and Considerations

3.1. Receiver Design Trends

In this section, we will present a survey of low power receivers that have been published in top journals and conferences since 2005 [13]. The survey summarizes the state-of-the-art receiver specifications, helps identify the research directions and trends and gives a deep understanding of radio design trade-offs and limitations [21]. Figure 6a shows the power trend of published receivers over years. It can be seen that the first sub-µW receiver was introduced in 2012 [22] and, since then, a number of sub-µW wakeup receivers have been published for IoT applications.

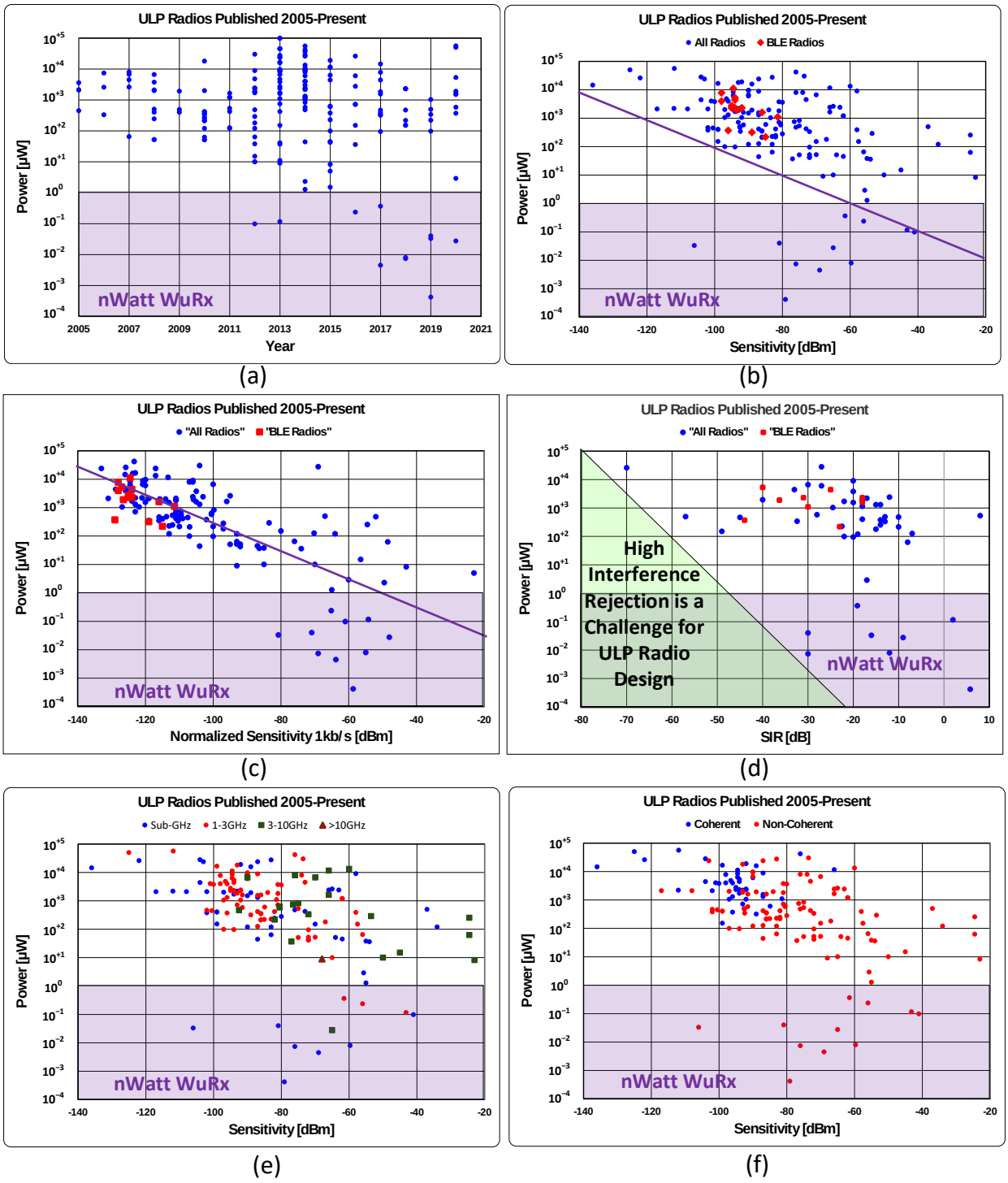

Figure 6. ULP (ultra-low power) receivers' survey showing different design trade-offs. (**a**) Power trend of published receivers over years; (**b**) power consumption versus sensitivity; (**c**) power consumption versus normalized sensitivity; (**d**) power versus signal-to-interference ratio (SIR); (**e**) power versus sensitivity at different frequency ranges; and (**f**) power versus sensitivity for different modulation schemes.

An important figure of merit (FoM) in receivers design is based on the product of power consumption and the achieved sensitivity. Lower FoM implies an energy-efficient radio design. However, since different radios target different data rate requirements, a normalized sensitivity on data rate is mandatory for a fair comparison and consistent FoM. Figure 6b shows the well known tradeoff between sensitivity and active power

consumption in radios. With the exception of sub-μW receivers, a Pareto optimal line with a slope of $-10\times/20$ dB can be observed bounding the power-sensitivity design space. The slope indicates that for every 20 dB improvement in sensitivity (or a $10\times$ increase in the transmission range in free-space), you would expect $10\times$ increase in the power. Therefore, in order to achieve a lower power operation, sensitivity shall be sacrificed. Normalizing the sensitivity to data rate for each point, as shown in Figure 6c, results in a clearer observation for the power-sensitivity trade-off since sub-μW receivers typically operate at fairly low data-rates.

The signal-to-interference ratio (SIR) is another performance metric which resembles another challenge to achieve robust operation at a limited power budget. Figure 6d clearly shows the aforementioned trade-off. Another important observation is that few papers report the SIR performance with a modulated interferer and the majority of these ULP radios have power consumption of 100 s of μWs. The reason is that in order to achieve good rejection at adjacent channels, frequency translation and cascaded signal filter stages are required which translates to higher power consumption. An alternative approach to improve the frequency selectivity of the receiver is based on exploiting high-Q off-chip RF MEMS filters, as in [23,24]. However, it lowers the system integration level and increases the module's cost. In addition, it requires multiple devices to cover the wide bandwidth required in many standards. Network level solutions such as frequency-hopping can effectively improve interference tolerance as proposed in [16].

The distribution of ULP receivers across different frequency bands is shown in Figure 6e. As can be seen, sub-10 μW receivers operate at sub-3 GHz frequency range. Lower frequencies provide wider coverage at the expense of data rates which is attractive in numerous IoT applications. Several low power and low voltage techniques can be utilized at low frequencies like subthreshold analog and digital logic to reach <1 μW power budget [20].

Complexity of the modulation is another critical factor which limits the power consumption of the receivers [25] as depicted in in Figure 6f. Coherent modulation schemes (e.g., BPSK, OFDM, QAM) require the phase information of the received signal for proper demodulation and hence high-performance PLLs are used. This results in higher power consumption for demodulation. On the other hand, simple modulation schemes like OOK and FSK are suitable for ultra-low power designs. All sub-μW receivers utilize non-coherent modulation schemes. Additionally, simple modulation combined with low data rate allows the implementation of bit-level duty-cycling to further reduce the power consumption as reported in [26]. Thus, decent sensitivity levels at low average power consumption can be achieved at the expense of the data rate.

Fully-compliant BLE receivers tend to consume several mWs of power. This is expected due to the stringent requirements on sensitivity at high data rates, adjacent channel interference rejection, GFSK modulation error and center frequency deviation. To achieve these specifications, power-hungry circuit blocks as high-gain LNAs, high-selectivity active filters, high-performance PLLs and accurate and fast-startup reference oscillators are required.

The survey also provides a holistic overview of the common receiver architectures and circuit techniques followed in ULP radio design as summarized in Figure 7. Since the power consumption scales with frequency, RF gain and selectivity consume a large portion of the receiver power profile. Since RF power consumption dominates the power budget, employing passive RF front-ends significantly decreases the overall RX's power consumption. In sub-μW receivers, RF envelope detectors (ED), e.g., diodes, preceded by high-Q transformers are commonly used with moderate sensitivity performance [20]. In such architectures, the interference rejection techniques are mostly focused on continuous wave tones which are not an accurate assumption since wireless communication is packetized, resulting in discontinuous interference. In addition, many modulation formats result in amplitude variation making those techniques inefficient in real-world scenarios

due to multipath fading. ED-based receivers are adequate mainly at low frequency ranges because of their large parasitic capacitors [27].

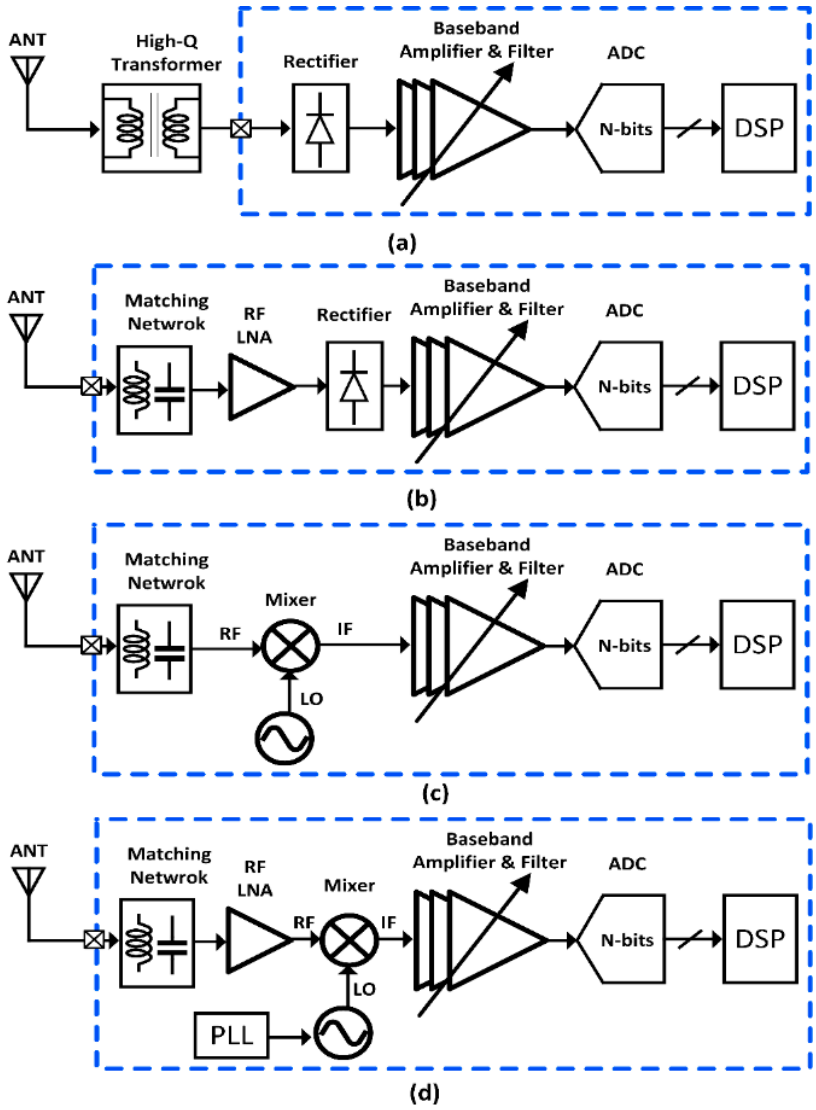

Figure 7. Common architectures of low power receivers: (**a**) energy-detector first; (**b**) energy-detector + LNA first; (**c**) mixer-first without PLL; (**d**) LNA-first architectures.

Mixer-first receivers are another attractive solution to avoid power-hungry active RF gain [28–33]. Passive N-path mixers are utilized as a first stage and are matched to the antenna. However, mixer-first architectures exhibit higher noise figure compared to LNA-first receivers, limiting their sensitivity. Nevertheless, mixer-first architectures can still achieve decent sensitivity levels through passive gain provided by matching networks in sub-mW receivers [34]. In such architectures, the major part of power is consumed by the LO generation and buffers used to drive the mixer switches. Different techniques are proposed to decrease the power of LC-based LO generation including utilizing high-Q low profile off-chip inductors which can be integrated with the radio in the same package. This solution results in a 75% power saving compared to on-chip LC oscillators at the expense of integration level [35]. Alternatively, ring-oscillators (RO) can be exploited for low-power LO generation especially in advanced CMOS nodes. The main challenge becomes improving the frequency stability and phase noise performance of the RO to avoid the degradation in the sensitivity and/or selectivity of the receiver [16].

Table 1 summarizes the trade-off between power and other performance metrics in BLE receivers. The table shows the performance of back-channel BLE receivers in comparison with fully-compliant BLE receivers [36–47]. It can be seen that state-of-the-art fully compliant receivers consume around ~2 mW, while BLE back-channel receivers have power consumption as low as ~200 µW. The receiver data rate, sensitivity at BER of 0.1% and adjacent channel rejection are lower in the case of back-channel BLE receivers which can be acceptable for some targeted applications. To sum up, there is still a room for innovation to improve the performance of low power radios.

Table 1. Comparison table for the state-of-the-art Bluetooth-Low Energy receivers.

	[12] JSSC'21	[16] JSSC'19	[39] RFIC'18	[18] CICC'18	[46] ISSCC'20	[47] ISSCC'20	[40] ISSCC'18
Standard	BLE WuRx	BLE B.C.	BLE B.C.	BLE B.C.	BLE4.0	BLE4.0/5.0	BLE4.0/5.0
Technology	65 nm	40 nm	65 nm	65 nm	40 nm	22 nm	40 nm
Supply Voltage	0.5 V	1.0/0.9 V	1.1/0.9 V	0.75 V	0.9/1.0 V	0.5 V	0.8 V
Modulation	FSK: 3-channel voting + pkt length + pkt interval + RSSI	FSK: 3-channel hopping sequence + BC symbol correlation		GFSK w/data repetition	GFSK	GFSK	GFSK
Data Rate	N/A	250 kbps	112.5 kbps	333 kbps	1 Mbps	1/2 Mbps	1/2 Mbps
Latency	1 adv. packet ~200 µs	1 adv. event 1.47 ms		1 adv. packet ~200 µs	N/A	N/A	N/A
RX Sensitivity	−85 dBm	−82.2 dBm	−57.5 dBm	−76.6 dBm	−86 dBm	−96.4 dBm	−95 dBm
Power Consumption	220 µW	1200 µW	150 µW	230 µW	2100 µW	1900 µW	3040 µW
SIR [dB] @2 MHz	−6 dB	−10 dB	−4 dB	N/A	−18 dB	−36.1 dB	−18 dB
Die Area	2.4 mm^2	1 mm^2	1.1 mm^2	4 mm^2	1.3 mm^2	1.9 mm^2	0.8 mm^2

3.2. Transmitter Design Trends

A generic architecture of a BLE transmitter is shown in Figure 8, summarizing the main blocks referred to in this section. The following design trends are observed in recent BLE transmitter publications.

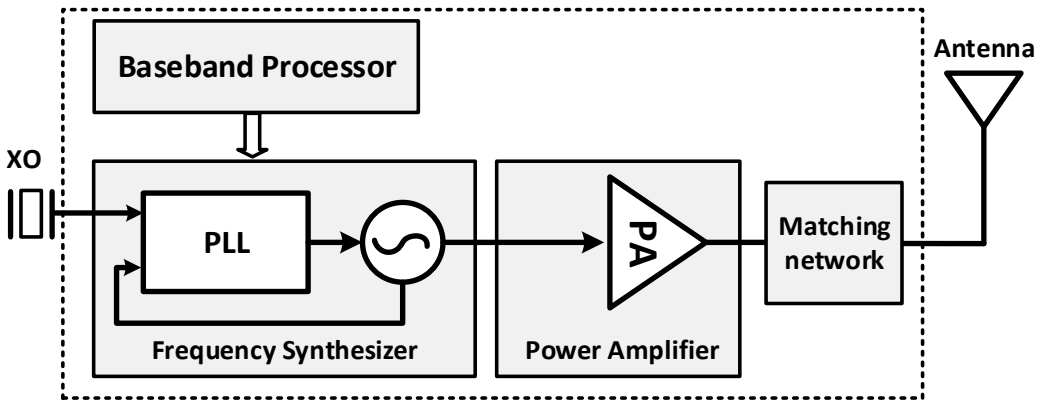

Figure 8. Conventional architecture of BLE transmitters.

3.2.1. Direct GFSK Modulation for Open-Loop LCVCO

BLE utilizes GFSK as its modulation scheme for data transmission. Traditionally, 2-point injection in the PLL is used to modulate the output frequency while the PLL is locked [10,37,48,49]. The digital baseband of the BLE transmitter generates control signals according to the data packet and injects the corresponding frequency control words to the PLL reference and the VCO at the same time. In this way, by balancing the reference phase and the VCO phase at the same time, the frequency change in the VCO output will not cause a transient signal in the loop for the PLL during transmission. However, this topology requires matched control at both of the injection points and it is easily affected by the PLL bandwidth, data rate and frequency deviation according to the BLE standards. Recently, it was discovered that typical LC-VCOs can easily satisfy the phase noise requirement of the BLE standard while running open loop [50]. More and more designs have started to utilize direct frequency modulation on an open-loop VCO [5,6,51–53]. This calibration and open loop modulation method has several benefits compared to the traditional modulation method: (1) it simplifies the role of the PLL in the BLE transmitter and reduce its design complexity, (2) it could reduce the average power consumption of the transmitter by duty cycling the PLL and (3) it enables new design methodologies for BLE transmitters such as crystal-less design.

3.2.2. Digitization of BLE Transmitters

Another trend of BLE transmitter design is digitization. There are three major building blocks in a BLE transmitter: baseband processor, frequency synthesizer and power amplifier (PA). The baseband processor is a digital block that generates data packets for modulation and transmission. The frequency synthesizer converts the baseband signal into RF frequency at its target channel and applies modulation to the data. In addition, finally, the PA amplifies the signal for transmission. All-digital PLLs have been used more and more in recent designs [37,51,52]. Due to CMOS process scaling, digitally controlled capacitor banks can now reach very fine resolution. Thus, the modulation signal, which used to be applied to the varactor in the LC-VCO in the analog charge pump PLL, is now applied to these digitally controlled capacitor banks in the ADPLL [37]. Recently, [54] proposed the first reported ring-oscillator based all-digital BLE transmitter design which has successfully removed the LC-VCO as the last analog circuit block in the frequency synthesizer block. The power amplifier has also gone digital as well. The class-D switched-capacitor digital power amplifier [55] has been adopted more and more in recent publications. Digital architectures benefit more from process scaling and could eventually be automatically synthesized using digital IC design tools [56]. This will result in significant reduction in production time and overall cost for circuit design.

3.2.3. Reduction of On-Chip/Off-Chip Components

In order to reduce the overall cost of the BLE module, a lot of research has been done to reduce the on-chip and off-chip components. In the past decade, a lot of the research focused on reducing the number of passive devices in the matching networks. Ref. [10] proposed a BLE transceiver with embedded RX image-rejection filter and TX harmonic-suppression filter by reusing an on-chip matching network that reduced the number of passive devices. Ref. [53] proposed a BLE transmitter utilizing a co-designed loop antenna and combined enhanced power oscillator which embedded the matching network into the power oscillator while improving both the VCO phase noise and transmitter efficiency. These designs reduced the number of on chip inductors which typically occupy a large portion of the die area. As mentioned above, the all-digital BLE transmitter design proposed in [50,54] replaced the LC-VCO with an ultra-low power ring oscillator and successfully removed all the inductors from the transmitter, resulting in a 40× core area saving compared to the state-of-the-art.

Recent work focuses on removing the crystal oscillator (XO) in BLE transmitters [57–59]. The XO is one of the most expensive off-chip components in a BLE module. Several XO

replacements have been evaluated, such as a real time clock (RTC), FBAR oscillator and recovered RF signal. In [57], the high-frequency XO is replaced with a 32 kHz real-time clock (RTC) for frequency calibration and channel selection, while in [58], the XO is replaced with an FBAR resonator. The work in [46,58] reported an XO-less BLE transmitter with clock recovery from GFSK-modulated BLE packets. These designs show that the BLE transmitter is capable of working without a typical MHz-range XO and it not only reduces the overall cost of the BLE module but also introduces some new design insights for BLE beacon transmitters.

3.2.4. Transmitter-Focused Design Requirement for System Efficiency

The brief survey below summarizes recent design trends in ultra-low power BLE transmitter designs. In order to reduce power consumption as well as the overall cost and improve the system efficiency, a lot of techniques are used for different applications. In order to design the BLE transmitter at its physical limit in terms of power and cost, designers have to adjust their design specifications according to application needs. For example, the frequency synthesizer specifications in traditional full function BLE transceivers are set by the receiver adjacent channel rejection requirements which requires exceptional performance of the VCO. However, from the transmitter's point of view, such performance far exceeds its need according to either spectrum emission or frequency modulation requirement [50,54,60]. Thus, designing the transmitter frequency synthesizer for a BLE network according to the receiver requirement is wasting power and cost. For power amplifier design in BLE transmitters, it is better to optimize the output power and system efficiency according to application needs as well. For example, if the target communication range is only within 3–4 m, optimizing the PA for its highest efficiency at 10 dBm would not be as efficient as optimizing its highest efficiency at 0 dBm.

Table 2 presents a comparison table for state-of-the art BLE transmitters with different architectures. It can be seen that BLE transmitters have an average overall efficiency around 25%. Therefore, in order to achieve longer transmission range, the power consumption is expected to be in mW levels. Aggressive duty-cycling techniques can be implemented for discontinuous transmission events/advertisements to bring the average power consumption to µW levels for ULP applications.

Table 2. Comparison table for the state-of-the-art Bluetooth-Low Energy transmitters.

	[59] JSSC'21	[53] ISSCC'19	[6] JSSC'19	[53] JSSC'19	[41] ISSCC'18	[51] JSSC'16
Technology	40 nm	65 nm	28 nm	40 nm	65 nm	28 nm
Supply Voltage	0.6/1.0 V	1.2 V	0.2 V	0.6/0.9 V	1.0 V	0.5/1.0 V
Transmission Scheme	Closed loop (RO-based)	Open Loop	Closed loop (Type-I)	Closed loop (RO-based)	Closed loop (ADPLL)	Closed loop (PLL)
PLL Locking Time	50 µs	15 µs	N/A	0.4 µs	Not reported	15 µs
Power Consumption	1.1 mW	0.61 mW	4 mW	1.55 mW	3.1 mW	6.3 mW
TX Output Power	Not reported	−8.4 dBm	0 dBm	−3.3 dBm	−3 dBm	3 dBm
Overall efficiency	Not reported	23.6%	25%	30.17%	16.13%	32%
Die Area	1.33 mm^2	0.494 mm^2	0.53 mm^2	0.0166 mm^2	1.64 mm^2 *	0.65 mm^2

* Transmitter and receiver area.

4. Conclusions and Future Work

BLE, as a well-established protocol, is utilized for short-range communications in a wide spectrum of applications, ranging from audio streaming to wireless sensors nodes. It offers a low power solution that can support connectivity between heterogeneous IoT devices and access points in personal area networks. Several efforts have been devoted

to reducing the power consumption of the RF radios to empower scaling IoT devices and enable self-powered operation. Efficient and complete solutions can be realized in both the network and physical layers. In the network layer, back-channel communication is presented where the back-channel message is embedded in a standard compliant BLE packets which is an attractive solution to design ULP radios while able to connect with the already-deployed infrastructure. Back-channel communication can be implemented in a packet-level fashion within an advertisement event or within a packet based on the latency requirements. This approach allows the main radios to stay in a deep sleep-mode, while the ULP wakeup/BC receivers continuously monitors the spectrum for wakeup/BC signaling from the access points or other fully functioning devices.

We presented a comprehensive survey for fully compliant BLE transceivers as well as back-channel receivers. In receive mode, fully compliant BLE receivers consume mWs of power to meet the stringent requirements on the data rate, sensitivity level at 0.1% BER and adjacent channel interference rejection. On the other hand, different backchannel receiver architectures were proposed to limit the power consumption to 10 s or 100 s of µWs. Mixer-first architectures, in an open-loop transmission scheme, accompanied with RF passive gain provide a decent performance at low power budget. BLE transmitters utilizing linear/switched power amplifiers suffer from low overall efficiency which led to a power consumption of several mWs to achieve high output power levels. Ring oscillator PLL-based architectures are proven to decrease the power budget to 100 s of µWs while satisfying the BLE requirements in terms of phase noise and frequency stability. Alternatively, open loop transmission utilizing LC-based oscillators can be utilized to eliminate the extra power of PLLs and PAs leading to a significant reduction in power consumption.

Extensive research efforts from industry and academia are still ongoing to create more energy-efficient wireless connectivity and low-power radio design architectures. These efforts extend beyond the BLE standard to cover the entire connectivity landscape of IoT devices.

Funding: This research was supported by the Advanced Self-Powered Systems of Integrated Sensors and Technologies (ASSIST), a Nano-Systems Engineering Research Center funded by National Science Foundation, grant number EEC1160483.

Informed Consent Statement: Not applicable.

Data Availability Statement: Publicly available datasets were analyzed in this study. This data can be found here: https://wics.engin.umich.edu/ultra-low-power-radio-survey/.

Conflicts of Interest: The authors declare no conflict of interest.

References

1. Jeon, K.; She, J.; Soonsawad, P.; Ng, P. BLE Beacons for Internet of Things Applications: Survey, Challenges, and Opportunities. *IEEE Internet Things J.* **2018**, *5*, 811–828. [CrossRef]
2. Bechthum, E.; Dijkhuis, J.; Ding, M.; He, Y.; Van Den Heuvel, J.; Mateman, P.; Van Schaik, G.; Shibata, K.; Song, M.; Tiurin, E.; et al. 30.6 A Low-Power BLE Transceiver with Support for Phase-Based Ranging, Featuring 5 µs PLL Locking Time and 5.3 ms Ranging Time, Enabled by Staircase-Chirp PLL with Sticky-Lock Channel-Switching. In Proceedings of the IEEE International Solid-State Circuits Conference—(ISSCC), San Francisco, CA, USA, 2–6 February 2020; pp. 470–472.
3. Moosavifar, M.; Wentzloff, D. Analysis of Design Trade-Offs in Ultra Low Power FSK Receivers for Phase-Based Ranging. In Proceedings of the IEEE Topical Conference on Wireless Sensors and Sensor Networks (WiSNeT), San Diego, CA, USA, 23 January 2021.
4. Zhang, H.; Wentzloff, D.; Kim, H. Software-Defined, WiFi and BLE Compliant Back-Channel for Ultra-Low Power Wireless Communication. In Proceedings of the IEEE Global Communications Conference (GLOBECOM), Washington, DC, USA, 4–8 December 2016; pp. 1–6.
5. Abdelatty, O.; Bishop, H.; Shi, Y.; Chen, X.; Alghaihab, A.; Calhoun, B.; Wentzloff, D. A Low Power Bluetooth Low-Energy Transmitter with a 10.5 nJ Startup-Energy Crystal Oscillator. In Proceedings of the IEEE 45th European Solid State Circuits Conference (ESSCIRC), Cracow, Poland, 23–26 September 2019; pp. 377–380.
6. Yang, S.; Yin, J.; Yi, H.; Yu, W.; Mak, P.; Martins, R. A 0.2-V Energy-Harvesting BLE Transmitter With a Micropower Manager Achieving 25% System Efficiency at 0-dBm Output and 5.2-nW Sleep Power in 28-nm CMOS. *IEEE J. Solid-State Circuits* **2019**, *54*, 1351–1362. [CrossRef]

7. Ruiz, L.; Ridder, M.; Fan, D.; Gong, J.; Li, B.; Mills, A.; Cobarrubias, E.; Strohmaier, J.; Jur, J.; Lach, J. Self-Powered Cardiac Monitoring: Maintaining Vigilance with Multi-Modal Harvesting and E-Textiles. *IEEE Sens. J.* **2021**, *21*, 2263–2276. [CrossRef]
8. Li, S.; Breiholz, J.; Kamineni, S.; Im, J.; Wentzloff, D.; Calhoun, B. An 85 nW IoT Node-Controlling SoC for MELs Power-Mode Management and Phantom Energy Reduction. In Proceedings of the IEEE International Symposium on Circuits and Systems (ISCAS), Seville, Spain, 6–9 September 2020; pp. 1–5.
9. Chen, G.; Ghaed, H.; Haque, R.; Wieckowski, M.; Kim, Y.; Kim, G.; Fick, D.; Kim, D.; Seok, M.; Wise, K.; et al. A cubic-millimeter energy-autonomous wireless intraocular pressure monitor. In Proceedings of the IEEE International Solid-State Circuits Conference (ISSCC), San Francisco, CA, USA, 20–24 February 2011; pp. 310–312.
10. Sano, T.; Mizokami, M.; Matsui, H.; Ueda, K.; Shibata, K.; Toyota, K.; Saitou, T.; Sato, H.; Yahagi, K.; Hayashi, Y. 13.4 A 6.3 mW BLE transceiver embedded RX image-rejection filter and TX harmonic-suppression filter reusing on-chip matching network. In Proceedings of the IEEE International Solid-State Circuits Conference (ISSCC), San Francisco, CA, USA, 22–26 February 2015; pp. 1–3.
11. Hanes, D.; Salgueiro, G.; Grossetete, P.; Barton, R.; Henry, J. *IoT Fundamentals: Networking Technologies, Protocols, and Use Cases for the Internet of Things*; Cisco Press: Indianapolis, IN, USA, 2017; ISBN 9780134307091.
12. Wang, P.; Mercier, P. An Interference-Resilient BLE-Compatible Wake-Up Receiver Employing Single-Die Multi-Channel FBAR-Based Filtering and a 4-D Wake-Up Signature. *IEEE J. Solid-State Circuits* **2021**, *56*, 416–426. [CrossRef]
13. Wentzloff, D. Low Power Radio Survey. Available online: www.eecs.umich.edu/wics/low_power_radio_survey.html (accessed on 30 March 2021).
14. Kim, H.; Wentzloff, D. Back-Channel Wireless Communication Embedded in WiFi-Compliant OFDM Packets. *IEEE J. Sel. Areas Commun.* **2016**, *34*, 3181–3194. [CrossRef]
15. Im, J.; Kim, H.; Wentzloff, D. A 335 μW −72 dBm receiver for FSK back-channel embedded in 5.8 GHz Wi-Fi OFDM packets. In Proceedings of the IEEE Radio Frequency Integrated Circuits Symposium (RFIC), Honolulu, HI, USA, 4–6 June 2017; pp. 176–179.
16. Alghaihab, A.; Shi, Y.; Breiholz, J.; Kim, H.; Calhoun, B.; Wentzloff, D. Enhanced Interference Rejection Bluetooth Low-Energy Back-Channel Receiver With LO Frequency Hopping. *IEEE J. Solid-State Circuits* **2019**, *54*, 2019–2027. [CrossRef]
17. Brown, J.; Huang, K.; Ansari, E.; Rogel, R.; Lee, Y.; Wentzloff, D. An ultra-low-power 9.8 GHz crystal-less UWB transceiver with digital baseband integrated in 0.18 μm BiCMOS. In Proceedings of the IEEE International Solid-State Circuits Conference (ISSCC), San Francisco, CA, USA, 17–21 February 2013; pp. 442–443.
18. Abdelhamid, M.; Paidimarri, A.; Chandrakasan, A. A −80 dBm BLE-compliant, FSK wake-up receiver with system and within-bit dutycycling for scalable power and latency. In Proceedings of the IEEE Custom Integrated Circuits Conference (CICC), San Diego, CA, USA, 8–11 April 2018; pp. 1–4.
19. Tang, S.; Yomo, H.; Takeuchi, Y. Optimization of Frame Length Modulation-Based Wake-Up Control for Green WLANs. *IEEE Trans. Veh. Technol.* **2015**, *64*, 768–780. [CrossRef]
20. Roberts, N.; Craig, K.; Shrivastava, A.; Wooters, S.; Shakhsheer, Y.; Calhoun, B.; Wentzloff, D. 26.8 A 236 nW −56.5 dBm-sensitivity Bluetooth low-energy wakeup receiver with energy harvesting in 65 nm CMOS. In Proceedings of the IEEE International Solid-State Circuits Conference (ISSCC), San Francisco, CA, USA, 31 January–4 February 2016; pp. 450–451.
21. Roberts, N.; Wentzloff, D. A 98 nW wake-up radio for wireless body area networks. In Proceedings of the IEEE Radio Frequency Integrated Circuits Symposium, Montreal, QC, Canada, 17–19 June 2012; pp. 373–376.
22. Wentzloff, D.; Alghaihab, A.; Im, J. Ultra-Low Power Receivers for IoT Applications: A Review. In Proceedings of the IEEE Custom Integrated Circuits Conference (CICC), Boston, MA, USA, 22–25 March 2020; pp. 1–8.
23. Moody, J.; Dissanayake, A.; Bishop, H.; Lu, R.; Liu, N.; Duvvuri, D.; Gao, A.; Truesdell, D.; Barker, N.; Gong, S.; et al. A −106 dBm 33 nW Bit-Level Duty-Cycled Tuned RF Wake-up Receiver. In Proceedings of the Symposium on VLSI Circuits, Kyoto, Japan, 9–14 June 2019; pp. C86–C87.
24. Wang, P.; Mercier, P. 28.2 A 220 μW −85 dBm Sensitivity BLE-Compliant Wake-up Receiver Achieving −60 dB SIR via Single-Die Multi- Channel FBAR-Based Filtering and a 4-Dimentional Wake-Up Signature. In Proceedings of the IEEE International Solid-State Circuits Conference—(ISSCC), 17–21 February 2019; pp. 440–442.
25. Alghaihab, A.; Kim, H.; Wentzloff, D. Analysis of Circuit Noise and Non-Ideal Filtering Impact on Energy Detection Based Ultra-Low-Power Radios Performance. *IEEE Trans. Circuits Syst. II Express Briefs* **2018**, *65*, 1924–1928. [CrossRef]
26. Dissanayake, A.; Bishop, H.; Moody, J.; Muhlbauer, H.; Calhoun, B.; Bowers, S. A Multichannel, MEMS-Less −99 dBm 260nW Bit-Level Duty Cycled Wakeup Receiver. In Proceedings of the IEEE Symposium on VLSI Circuits 2020, Honolulu, HI, USA, 13–19 June 2020; pp. 1–2.
27. Moody, J.; Bowers, S. Triode-mode Envelope Detectors for Near Zero Power Wake-up Receivers. In Proceedings of the IEEE MTT-S International Microwave Symposium (IMS), Boston, MA, USA, 4–6 June 2019; pp. 1499–1502.
28. Kosari, A.; Moosavifar, M.; Wentzloff, D. A 152 μW −99 dBm BPSK/16-QAM OFDM Receiver for LPWAN Applications. In Proceedings of the IEEE Asian Solid-State Circuits Conference (A-SSCC), Tainan, Taiwan, 5–7 November 2018; pp. 303–306.
29. Bryant, C.; Sjoland, H. A 0.55 mW SAW-Less Receiver Front-End for Bluetooth Low Energy Applications. *IEEE J. Emerg. Sel. Top. Circuits Syst.* **2014**, *4*, 262–272. [CrossRef]
30. Lee, S.; Choi, I.; Kim, H.; Kim, B. A Sub-mW Fully Integrated Wide-Band Receiver for Wireless Sensor Network. *IEEE Microw. Wirel. Compon. Lett.* **2015**, *25*, 319–321. [CrossRef]

31. Im, J.; Kim, H.; Wentzloff, D. A 217 μW −82 dBm IEEE 802.11 Wi-Fi LP-WUR using a 3rd- Harmonic Passive Mixer. In Proceedings of the IEEE Radio Frequency Integrated Circuits Symposium (RFIC), Philadelphia, PA, USA, 10–12 June 2018; pp. 172–175.
32. Rahman, M.; Harjani, R. A Sub-1-V 194- 31-dB FOM 2.3–2.5-GHz Mixer-First Receiver Frontend for WBAN with Mutual Noise Cancellation. *IEEE Trans. Microw. Theory Tech.* **2016**, *64*, 1102–1109. [CrossRef]
33. Abe, T.; Morie, T.; Satou, K.; Nomasaki, D.; Nakamura, S.; Horiuchi, Y.; Imamura, K. An ultra-low-power 2-step wake-up receiver for IEEE 802.15.4 g wireless sensor networks. In Proceedings of the Symposium on VLSI Circuits, Honolulu, HI, USA, 10–13 June 2014; pp. 1–2.
34. Im, J.; Kim, H.; Wentzloff, D. A 470 μW −92.5 dBm OOK/FSK Receiver for IEEE 802.11 WiFi LP-WUR. In Proceedings of the IEEE 44th European Solid State Circuits Conference (ESSCIRC), Dresden, Germany, 3–6 September 2018; pp. 302–305.
35. Salazar, C.; Cathelin, A.; Kaiser, A.; Rabaey, J. A 2.4 GHz Interferer-Resilient Wake-Up Receiver Using A Dual-IF Multi-Stage N-Path Architecture. *IEEE J. Solid-State Circuits* **2016**, *51*, 2091–2105. [CrossRef]
36. Masuch, J.; Delgado-Restituto, M. A 1.1-mW-RX -81.4-dBm Sensitivity CMOS Transceiver for Bluetooth Low Energy. *IEEE Trans. Microw. Theory Tech.* **2013**, *61*, 1660–1673. [CrossRef]
37. Liu, Y.; Bachmann, C.; Wang, X.; Zhang, Y.; Ba, A.; Busze, B.; Ding, M.; Harpe, P.; van Schaik, G.; Selimis, G.; et al. 13.2 A 3.7 mW-RX 4.4 mW-TX fully integrated Bluetooth Low-Energy/IEEE802.15.4/proprietary SoC with an ADPLL-based fast frequency offset compensation in 40nm CMOS. In Proceedings of the IEEE International Solid-State Circuits Conference—(ISSCC), San Francisco, CA, USA, 22–26 February 2015; pp. 1–3.
38. Kuo, F.; Ferreira, S.; Babaie, M.; Chen, R.; Cho, L.; Jou, C.; Hsueh, F.; Huang, G.; Madadi, I.; Tohidian, M.; et al. A Bluetooth low-energy (BLE) transceiver with TX/RX switchable on-chip matching network, 2.75 mW high-IF discrete-time receiver, and 3.6 mW all-digital transmitter. In Proceedings of the IEEE Symposium on VLSI Circuits (VLSI-Circuits), Honolulu, HI, USA, 15–17 June 2016; pp. 1–2.
39. Alghaihab, A.; Breiholz, J.; Kim, H.; Calhoun, B.; Wentzloff, D. A 150 μW −57.5 dBm-Sensitivity Bluetooth Low-Energy Back-Channel Receiver with LO Frequency Hopping. In Proceedings of the IEEE Radio Frequency Integrated Circuits Symposium (RFIC), Philadelphia, PA, USA, 10–12 June 2018; pp. 324–327.
40. Ding, M.; Wang, X.; Zhang, P.; He, Y.; Traferro, S.; Shibata, K.; Song, M.; Korpela, H.; Ueda, K.; Liu, Y.; et al. A 0.8 V 0.8 mm_2 bluetooth 5/BLE digital-intensive transceiver with a 2.3 mW phase-tracking RX utilizing a hybrid loop filter for interference resilience in 40 nm CMOS. In Proceedings of the IEEE International Solid—State Circuits Conference—(ISSCC), San Francisco, CA, USA, 11–15 February 2018; pp. 446–448.
41. Liu, H.; Sun, Z.; Tang, D.; Huang, H.; Kaneko, T.; Deng, W.; Wu, R.; Okada, K.; Matsuzawa, A. An ADPLL-centric bluetooth low-energy transceiver with 2.3 mW interference-tolerant hybrid-loop receiver and 2.9 mW single-point polar transmitter in 65nm CMOS. In Proceedings of the IEEE International Solid—State Circuits Conference—(ISSCC), San Francisco, CA, USA, 11–15 February 2018; pp. 444–446.
42. Sun, Z.; Liu, H.; Tang, D.; Huang, H.; Kaneko, T.; Wu, R.; Deng, W.; Okada, K. A 0.85 mm_2 BLE Transceiver with Embedded T/R Switch, 2.6 mW Fully-Passive Harmonic Suppressed Transmitter and 2.3 mW Hybrid-Loop Receiver. In Proceedings of the IEEE 44th European Solid State Circuits Conference (ESSCIRC), Dresden, Germany, 3–6 September 2018; pp. 310–313.
43. Yu, W.; Yi, H.; Mak, P.; Yin, J.; Martins, R. 24.4 A 0.18 V 382 μW bluetooth low-energy (BLE) receiver with 1.33 nW sleep power for energy-harvesting applications in 28 nm CMOS. In Proceedings of the IEEE International Solid-State Circuits Conference (ISSCC), San Francisco, CA, USA, 5–9 February 2017; pp. 414–415.
44. Thijssen, B.; Klumperink, E.; Quinlan, P.; Nauta, B. 30.4 A 370 μW 5.5 dB-NF BLE/BT5.0/IEEE 802.15.4-Compliant Receiver with >63 dB Adjacent Channel Rejection at >2 Channels Offset in 22 nm FDSOI. In Proceedings of the IEEE International Solid- State Circuits Conference—(ISSCC), San Francisco, CA, USA, 2–6 February 2020; pp. 466–468.
45. Park, B.; Kwon, K. 2.4-GHz Bluetooth Low Energy Receiver Employing New Quadrature Low-Noise Amplifier for Low-Power Low-Voltage IoT Applications. *IEEE Trans. Microw. Theory Tech.* **2021**, *69*, 1887–1895. [CrossRef]
46. Alghaihab, A.; Chen, X.; Shi, Y.; Truesdell, D.; Calhoun, B.; Wentzloff, D. 30.7 A Crystal-Less BLE Transmitter with −86 dBm Freq μ ency-Hopping Back-Channel WRX and Over-the-Air Clock Recovery from a GFSK-Modulated BLE Packet. In Proceedings of the IEEE International Solid- State Circuits Conference—(ISSCC), San Francisco, CA, USA, 11–15 February 2020; pp. 472–474.
47. Tamura, M.; Takano, H.; Shinke, S.; Fujita, H.; Nakahara, H.; Suzuki, N.; Nakada, Y.; Shinohe, Y.; Etou, S.; Fujiwara, T.; et al. 30.5 A 0.5 V BLE Transceiver with a 1.9 mW RX Achieving −96.4 dBm Sensitivity and 4.1 dB Adjacent Channel Rejection at 1 MHz Offset in 22 nm FDSOI. In Proceedings of the IEEE International Solid- State Circuits Conference—(ISSCC), San Francisco, CA, USA, 2–6 February 2020; pp. 468–470.
48. Staszewski, R.; Wallberg, J.; Rezeq, S.; Hung, C.-M.; Eliezer, O.; Vemulapalli, S.; Fernando, C.; Maggio, K.; Staszewski, R.; Barton, N.; et al. All-digital PLL and transmitter for mobile phones. *IEEE J. Solid-State Circuits* **2005**, *40*, 2469–2482. [CrossRef]
49. Prummel, J.; Papamichail, M.; Willms, J.; Todi, R.; Aartsen, W.; Kruiskamp, W.; Haanstra, J.; Opbroek, E.; Rievers, S.; Seesink, P.; et al. A 10 mW Bluetooth Low-Energy Transceiver with On-Chip Matching. *IEEE J. Solid-State Circuits* **2015**, *50*, 3077–3088. [CrossRef]
50. Chen, X.; Breiholz, J.; Yahya, F.; Lukas, C.; Kim, H.; Calhoun, B.; Wentzloff, D. Analysis and Design of an Ultra-Low-Power Bluetooth Low-Energy Transmitter with Ring Oscillator-Based ADPLL and 4× Frequency Edge Combiner. *IEEE J. Solid-State Circuits* **2019**, *54*, 1339–1350. [CrossRef]

51. Babaie, M.; Kuo, F.; Chen, H.; Cho, L.; Jou, C.; Hsueh, F.; Shahmohammadi, M.; Staszewski, R. A Fully Integrated Bluetooth Low-Energy Transmitter in 28 nm CMOS with 36% System Efficiency at 3 dBm. *IEEE J. Solid-State Circuits* **2016**, *51*, 1547–1565. [CrossRef]
52. Kuo, F.; Binsfeld Ferreira, S.; Chen, H.; Cho, L.; Jou, C.; Hsueh, F.; Madadi, I.; Tohidian, M.; Shahmohammadi, M.; Babaie, M.; et al. A Bluetooth Low-Energy Transceiver with 3.7-mW All-Digital Transmitter, 2.75-mW High-IF Discrete-Time Receiver, and TX/RX Switchable On-Chip Matching Network. *IEEE J. Solid-State Circuits* **2017**, *52*, 1144–1162. [CrossRef]
53. Shi, Y.; Chen, X.; Kim, H.; Blaauw, D.; Wentzloff, D. 28.3 A 606 µW mm-Scale Bluetooth Low-Energy Transmitter Using Co-Designed 3.5×3.5 mm_2 Loop Antenna and Transformer-Boost Power Oscillator. In Proceedings of the IEEE International Solid-State Circuits Conference—(ISSCC), San Francisco, CA, USA, 17–21 February 2019; pp. 442–444.
54. Chen, X.; Breiholz, J.; Yahya, F.; Lukas, C.; Kim, H.; Calhoun, B.; Wentzloff, D. A 486 µW All-Digital Bluetooth Low Energy Transmitter with Ring Oscillator Based ADPLL for IoT applications. In Proceedings of the IEEE Radio Frequency Integrated Circuits Symposium (RFIC), Philadelphia, PA, USA, 10–12 June 2018; pp. 168–171.
55. Yoo, S.; Walling, J.; Woo, E.; Jann, B.; Allstot, D. A Switched-Capacitor RF Power Amplifier. *IEEE J. Solid-State Circuits* **2011**, *46*, 2977–2987. [CrossRef]
56. Ajayi, T.; Kamineni, S.; Cherivirala, Y.; Fayazi, M.; Kwon, K.; Saligane, M.; Gupta, S.; Chen, C.; Sylvester, D.; Blaauw, D.; et al. An Open-source Framework for Autonomous SoC Design with Analog Block Generation. In Proceedings of the IFIP/IEEE 28th International Conference on Very Large Scale Integration (VLSI-SOC), Salt Lake City, UT, USA, 5–7 October 2020; pp. 141–146.
57. Li, C.; Yuan, M.; Liao, C.; Lin, Y.; Chang, C.; Staszewski, R. All-Digital PLL for Bluetooth Low Energy Using 32.768-kHz Reference Clock and ≤0.45-V Supply. *IEEE J. Solid-State Circuits* **2018**, *53*, 3660–3671. [CrossRef]
58. Wiser, B.; Sankaragomathi, K.; Schauer, J.; Korhummel, S.; Kavousian, P.; Yeager, D.; Arumugam, N.; Pletcher, N.; Barkin, D.; Parker, R.; et al. A 1.53 mm_3 crystal-less standards-compliant Bluetooth Low Energy module for volume constrained wireless sensors. In Proceedings of the Symposium on VLSI Circuits, Kyoto, Japan, 9–14 June 2019; p. 84.
59. Chen, X.; Alghaihab, A.; Shi, Y.; Truesdell, D.; Calhoun, B.; Wentzloff, D. A Crystal-Less BLE Transmitter with Clock Recovery From GFSK-Modulated BLE Packets. *IEEE J. Solid-State Circuits* **2021**, 1-1. [CrossRef]
60. Chen, X.; Kim, H.; Wentzloff, D. An analysis of phase noise requirements for ultra-low-power FSK radios. In Proceedings of the IEEE Radio Frequency Integrated Circuits Symposium (RFIC), Honolulu, HI, USA, 4–6 June 2017; pp. 37–40.